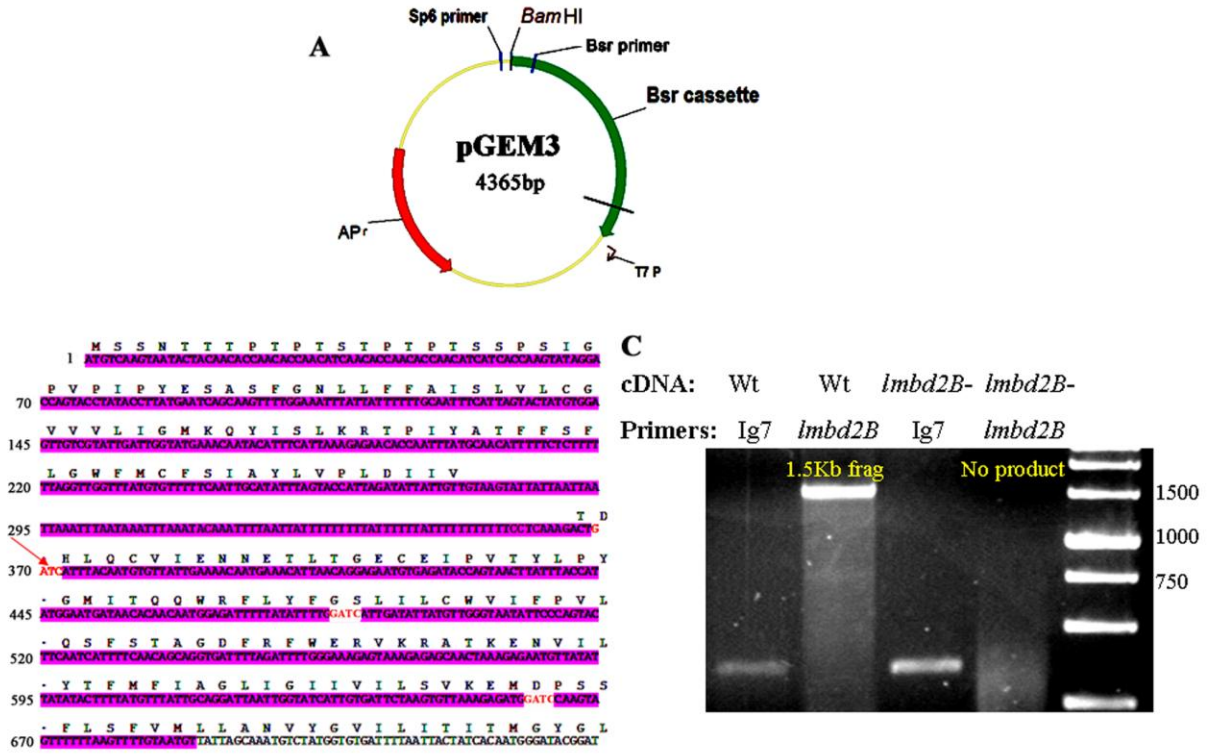

Supplementary Figure 1. The JSK1 mutant results from disruption of the lmbd2B gene. The *lmbd2B* knockout mutant generated using the recovered REMI plasmid does not produce an *lmbd2B* mRNA transcript.

In **A,** the pGEM3 plasmid used in REMI mutagenesis is shown**.** It contains a blasticidin resistant cassette (bsr). The BamHI site linearized for REMI is indicated. Also, the sites of the Sp6 and Bsr primers used for sequencing are labeled. In **B**, the *lmbd2B* nucleotide and amino acid sequence of a section of the coding region. A transcription start site is located at base number 1 and the stop site is at 2461. There is an intron at 278-366. DpnII sites are in red. The DpnII site of insertion is indicated with an arrow. The pink highlighted sequence (1-690) corresponds to the gene sequence obtained from sequencing the flanking DNA of the REMI plasmid insert from JSK1. In **C,** RNA from Wt and *lmbd2B*- cells was converted to cDNA and utilized in PCR. The first two lanes show cDNA from Wt cells. An Ig7 control gene transcript shows the presence of cDNA, and a 1.5Kb product of the expected size is produced with *lmbd2B* specific primers. The next two lanes show cDNA from *lmbd2B*- cells. No product is formed with the *lmbd2B* primers even though the Ig7 control gene transcript was made.

Supplementary Figure 2. A ClustalW alignment of LMBD2 sequences.

The LMBD2 protein sequences from *Homo sapiens* (Hs), *Xenopus laevis* (Xl), *Drosophila melanogaster* (Dm), *Nematostella vectensis* (Nv), *Caenorhabditis elegans* (Ce), and *Dictyostelium discoideum* (Dd) are aligned. Accession numbers are the same as in figure 2B. Grey shaded areas are predicted transmembrane domains and yellow shaded areas are predicted glycosylation sites.

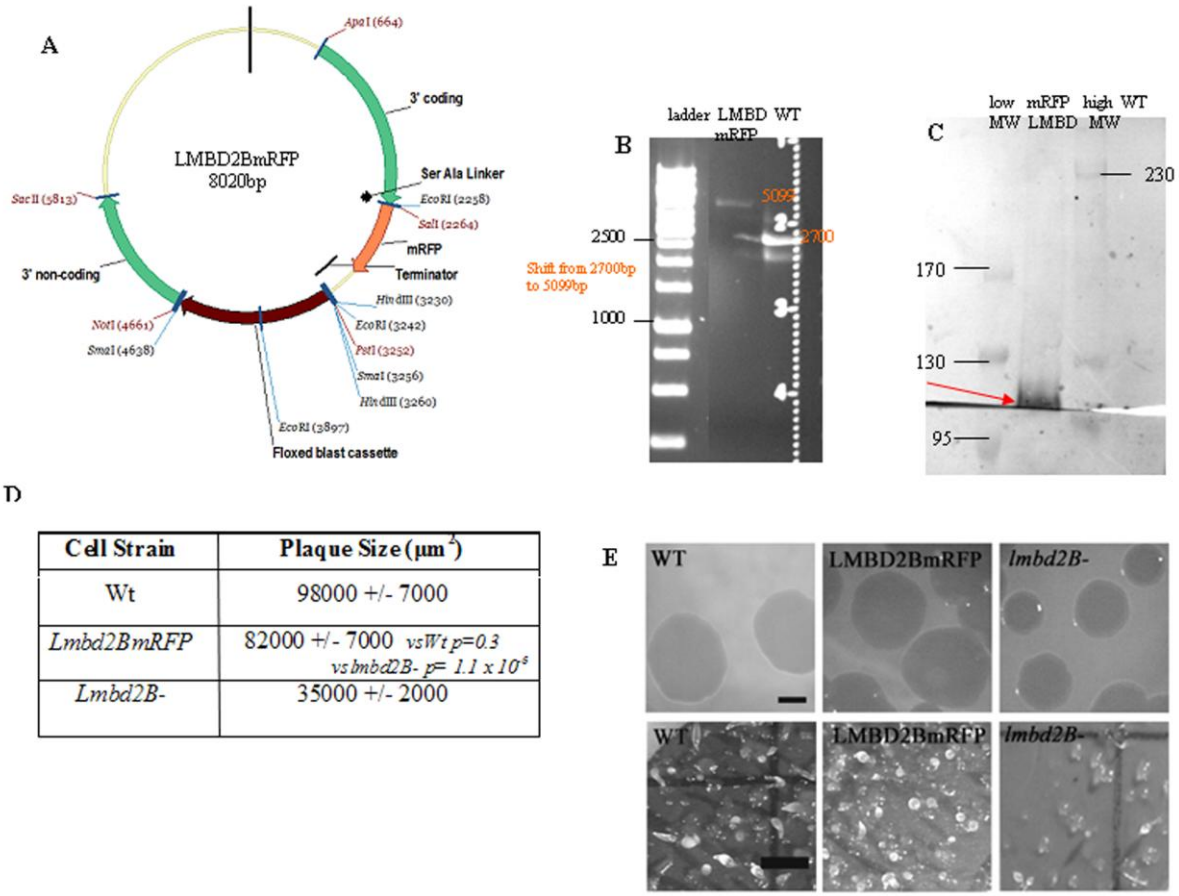

Cell Strain	Plaque Size (μm^2)
Wt	98000 +/- 7000
Lmbd2BmRFP	82000 +/- 7000 *vsWt p=0.3* *vs lmbd2B- p= 1.1 x 10⁻⁶*
Lmbd2B-	35000 +/- 2000

Supplementary figure 3. Creating the *lmbd2BmRFP* cell strain

A, a map of the *lmbd2B-mRFPmars* fusion construct is shown. The construct has 3' coding and non coding regions of the *lmbd2B* gene. A Ser-Ala linker immediately follows the coding region. After the linker mRFPmars is translated in frame with the coding region and a terminator sequence directly following the mRFPmars sequence. A bsr cassette with flanking lox p sites (for future removal by Cre recombinase) is present for selection. **Proper *lmbd2BmRFP* integration and protein production**

B, genomic PCR analysis showing correct insertion of the mRFP plasmid is shown. Primers flanking the expected mRFP insertions site were utilized. The mRFP construct is 2343 bps in length. In the *lmbd2BmRFP* cells there is about a 2300 bp shift in product size from the 2700 bp band found in the wild type strain to a 5000 bp band in the knock-in strain, indicating the correct insertion.

C shows a western blot using anti-mRFP primary antibody indicating a fusion protein of the correct size. The first lane is a low MW ladder, the second is $1x10^6$ LMBD2BmRFP cells, the

third lane is a high MW ladder, and the fourth is Wt control cells. The mRFP protein is 27 KDa, the LMBD2B protein is 89 KDa so the LMBD2BmRFP fusion product is expected to be about 116 KDa and is highlighted by a red arrow.

Results indicating normal function of the *lmbd2B-mRFP* fusion protein

D, cells were plated over *E.coli B/r*, and after 4 days images were taken and plaques measured. Wt and *lmbd2BmRFP* cells produce plaques that are similar in size and are not significantly different. The plaque sizes of *lmbd2BmRFP* are significantly larger than *lmbd2B*- cell plaques. These results suggest that the *lmbd2BmRFP* retains the Wt phenotype. **E** displays images of plaque sizes after 4 days (top row), and development on nitrocellulose filters after 24 hours (bottom row). The *Lmbd2BmRFP* knock in strain appears very similar to Wt cells in plaque formation and development. This is in contrast to *lmbd2b* null cells which show delayed and sparse development. The black scale bar represents 1000 μm.

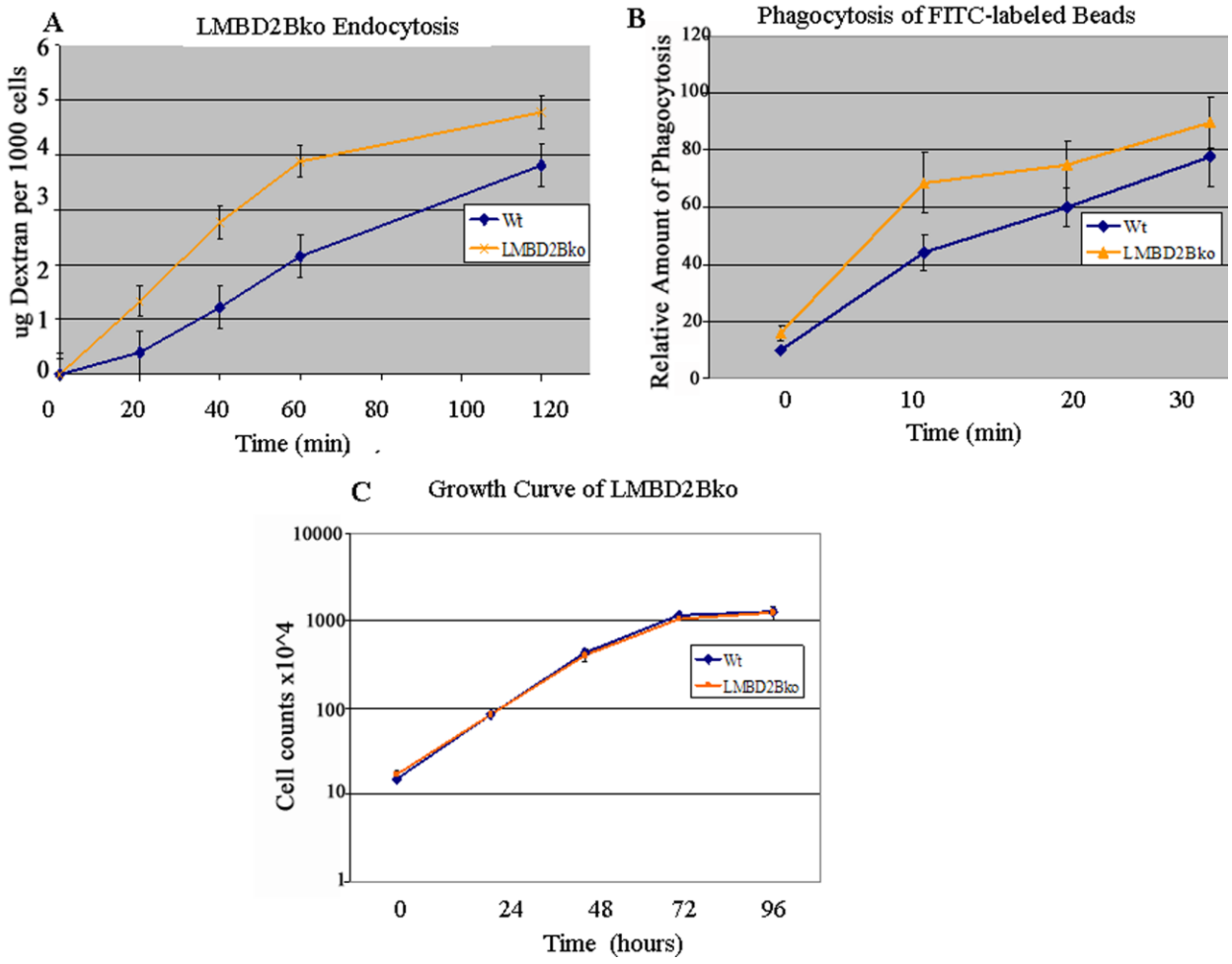

Supplementary figure 4. LMBD2B knockout effect on endocytosis, phagocytosis and growth.

In **A,** rates of endocytosis in the different cells types were measured based on the amount of FITC dextran uptake. The procedure was adapted from Brazill et al., 2001 (5). The rate of endocytosis of Wt and LMBD2B null cells were compared. There was an increase in endocytosis rates between Wt and LMBD2B null cells (N = at least 3 rounds). In **B**, phagocytosis was assayed by following the uptake of Carboxylated fluorescent latex beads (FITC#15702) from PolyScience, Warrenton Pa. (1um in diameter) as described by Witke et al., 1992 (63). The amount of phagocytosis was determined by the amount of fluorescence the cell ingested compared to the amount available. 100 percent relative phagocytosis is equal to complete ingestion of all beads in the solution. There was an increase in phagocytosis in

LMBD2B null cells (N = at least 6 measures for each time point). In **C**, cells were grown axenically and counts were taken starting at a low density (20 x 10^4) and continuing every 24 hours for 96 hours. The graph is exponential, each time point represents an additional 24 hours. There was no difference between the growth curve of LMBD2B null cells compared to Wt cells (N = at least 3 experiments).

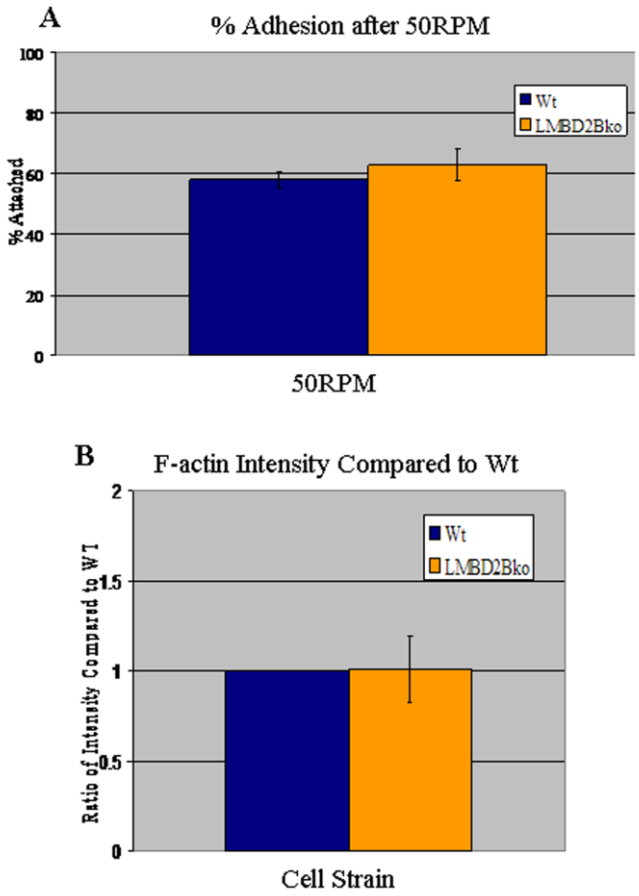

Supplementary figure 5. LMBD2B null cells show Wt levels of substrate adhesion and actin polymerization.

In **A,** substrate adhesion results are shown. Cells were placed on Petri dishes and allowed to adhere overnight. The cells were shaken at 50 RPM the next day for 45 minutes. The number of cells that detached after shaking was counted. The percentage of cells that remained attached after 45 minutes are depicted in the bar graph. N = At least 3 repeats.

B displays F-actin levels. Growing cells in log phase were placed on a coverslip to adhere. The cells were then fixed and stained with Alexa Fluor 488 phalloidin, which binds polymerized F-actin. The graph shows the intensity of LMBD2B null fluorescence compared to Wt intensity, which was calculated using ImageJ. The F actin levels are the same. N = 15+ cells from 3 rounds of actin staining.

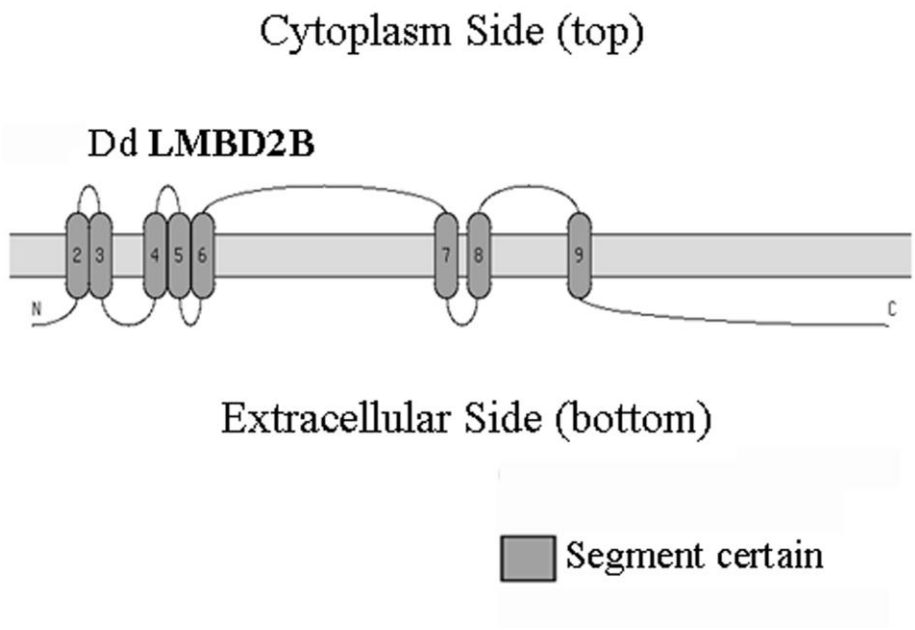

Supplementary Figure 6. Predicted topography of LMBD2B. The predicted topography of LMBD2B is shown. The program TopPred 0.01 was used to display the likely topography of LMBR1 receptors (9, 59). The transmembrane proteins are oriented such that cytoplasmic regions are on top and extracellular regions are on the bottom. The transmembrane segments are numbered. Since the N-terminus could be modeled as a transmembrane domain but with lower probability, the high probability transmembrane domain is number 2.

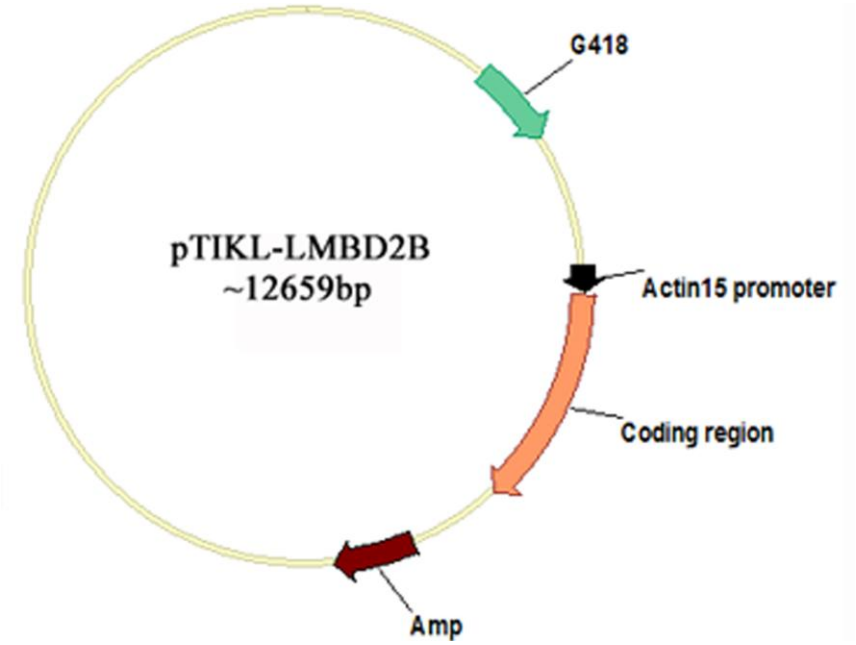

Supplementary Figure 7. LMBD2B rescue plasmid

The rescue plasmid was constructed from the pTIKL-MyD plasmid. It contains a G418 resistance cassette for selection and is driven by an actin 15 promoter. The full length LMBD2B cDNA has been inserted.